Permeability Performance and Antifouling Behavior of 3D Printed Chitosan/AgNP/GO Composite Membranes

Anthony C. Ogazi*[1] and Peter O. Osifo[1]

Abstract**—**Permeability performance and the antifouling characteristics of chitosan/silver nanoparticles/graphene oxide (CS/AgNP/GO) composite membranes modified with dimethyl acetamide (DMAc) were evaluated in this study. Appropriate integration of membrane components decreased the contact angle of the modified CS matrix, which improved fluid transport and hydrophilicity due to the strongly bound water oxygen-containing functional groups . The composite membranes exhibited improved thermal stability and fouling inhibition against bovine serum albumin (BSA) solute, achieving a remarkable flux recovery rate of 98.1%.

Keywords**—**Antifouling, hydrophilicity, modified chitosan, thermal stability

I. INTRODUCTION

Water is essential for all life, thriving ecosystems, energy production, food production, and sustainable development. Approximately two million people die annually from waterborne diseases transmitted by contaminated water sources or effluent because more than a billion people lack access to safe potable water and adequate sanitation [1]. Since a greater proportion of the population in developing nations relies solely on this water source, surface and waste water purification have become crucial for ensuring human sustainability and social advancement [2]. Membrane separation technology is utilized for a variety of water treatment applications, including biofouling control.

Chitosan (CS) is a fascinating biopolymer that is frequently used in membrane industries for water treatment because of its inherent antibacterial properties, biodegradability, and nontoxicity [3]. CS is also recognized as an antibacterial polysaccharide owing to the antimicrobial properties of the amino group of the glucosamine residue [4]. It is thought that chitosan's antibacterial activity comes from its cationic structure, which may interact with anionic components on the surface of microbial cells and mess up their metabolic processes [5]. Due to its many amino and hydroxyl groups, chitosan has also gotten a lot of attention as a powerful adsorbent for removing contaminants from water and effluent [6]. When combined chemically, chitosan (CS), silver nanoparticles (AgNP), and graphene oxide (GO) exhibit greater antibacterial activity than when used individually [7].

Therefore, the study carefully investigated the hydrophilicity and separation performance characteristics of chitosan/AgNP/GO composites against BSA molecules. The water contact angle measurements showed that adding DMAc to the CS matrix enhanced the thermal stability and wettability, while the printed membranes exhibited improved antifouling properties.

Anthony C. Ogazi*[1], is with the Chemical Engineering Department, Vaal University of Technology, P/Bag X021, Vanderbijlpark 1900, RSA

Peter O. Osifo[1], is with the Chemical Engineering Department, Vaal University of Technology, P/Bag X021,Vanderbijlpark 1900, RSA

II. METHODS

A. Preparation of modified CS ink formulation

The modified Tollens' approach was adopted to synthesize AgNP-GO nanocomposites. In this process, silver nitrate ($AgNO_3$) was made by directly reducing it with trisodium citrate ($C_6H_5O_7Na_3$) in the presence of graphene oxide (GO) in a solution. In the experiment, GO solution weighing 0.5 g was combined with 0.4 g of $AgNO_3$ and subjected to progressive stirring for duration of 60 minutes. A 50-milliliter solution of $C_6H_5O_7Na_3$ with a concentration of 0.5 moles per liter was gradually added drop by drop in order to complete the reduction procedure. After 24 hours of incubation, the solution underwent centrifugation and subsequent washing with a 98% ethanol-water solution. The resulting mixture was then subjected to drying in a vacuum oven, yielding graphene oxide-silver nanoparticles (GO-AgNP). Subsequently, 1 gram of CS was dissolved in an aqueous solution of 1% acetic acid (HAc) at room temperature. The resulting mixture was then subjected to vigorous stirring for 60 minutes. In order to achieve neutralization of the HAc, a volume of 0.5 ml of a 2% (w/v) NaOH solution was introduced into the mixture.

B. 3D printing of CS-GO-AgNP membranes

The modified CS fluid samples were thereafter printed using a Colorsun A1630 UV flatbed inkjet printer (China) equipped with two UV LED lights, and Acro RIP White version 9.0 print software. The modified CS fluid properties had been previously determined and adopted for this study to ensure adequate drop formation [8]. The printer uses Epson L805 drop-on-demand piezoelectric inkjet printhead. The pH of the solution was carefully adjusted to a value of 7 using a

https://doi.org/10.17758/IICBE5.C1123046

buffer solution in order to mitigate any harm to the inkjet 3D printhead.

III. RESULTS AND DISCUSSION

A. FT- IR analysis of modified CS composites

FT-IR analysis was used to determine the functional groups embedded in the modified CS composite membrane samples. As shown in Figure 1, all three composite samples displayed broad, robust peaks of O-H bond stretching between 3253 and 2932 cm^{-1}. This is likely due to bands of O-H in hydroxyl groups and bands of N-H in amino groups that overlap, both of which are responsible for O-H bond stretching [29]. The increase in DMAc concentration, as demonstrated by curve ‘b’ (CS 82 wt.%: 14 wt.%: GO-AgNP 4 wt.%), improved the O-H bond's intensity within the modified CS matrix.

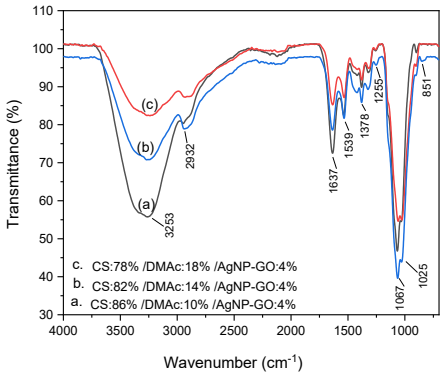

Fig 1: FT-IR analysis of the modified CS composite

Based on how aliphatic conjugated alkenes stretch in symmetric and asymmetric ways, the single peak at 1637 cm^{-1} may show how the alkene (C=C) bond is stretched. The extra stretching of the N-O bond at 1539 cm^{-1} could be a sign that nitro compounds are present because of the chemical interactions between CS and DMAc molecules. Since the band between 1380 cm^{-1} and 1240 cm^{-1} is caused by the bending of the O-H bond in primary alcohol, it can be shown that there is a hydrogen bond in CS-DMAc-GO/AgNP composites. Alkyl aryl ether bond (C-O) stretching intensity was strongest in curve C, which may imply that all of the constituent atoms may produce the best membrane performance. This stretching intensity was observed at 1255 cm^{-1}. The functional groups in the modified Chitosan filtration membranes can take different shapes. C-N stretching of amine in DMAc (1027–1020 cm^{-1}), C-H bending in CS–DMAc at 851 cm^{-1}, and C-O stretching of residual acetyl groups in CS (1720–1067 cm^{-1}) are all examples of these shapes. Because functional groups with oxygen and water are tightly bound to the modified Chitosan film, the typical band for AgNP attachment would be between 3250 and 3450 cm^{-1} (O-H stretching) and 1076 and 1025 cm^{-1} (C-O-C stretching).

B. XRD Characterization of modified CS membranes

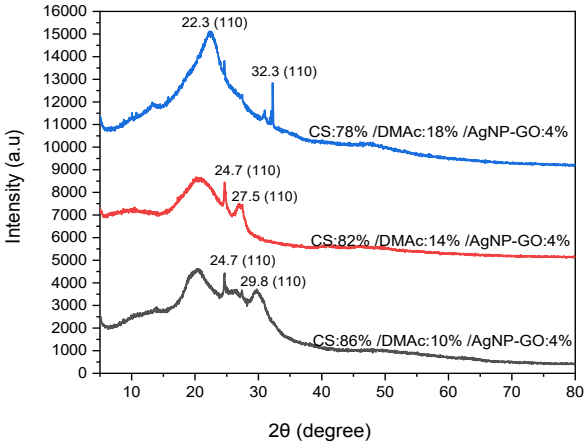

Fig 2**:** XRD patterns of the modified CS composites

Figure 2 shows the X-ray diffraction patterns of the samples. Most of the broad peak diffractions happen between the Bragg angle (2) of 20.0° and 35.0°, which is equivalent to 110 Ag crystal planes. This could mean that the amount of AgNP in the composite is consistent. The presence of AgNP in the CS matrix, however, resulted in the appearance of two large peaks at 224.7° and 29.8° for the modified membrane CS composite sample ‘a’ (CS 86%: DMAc 10%: AgNP/GO 4%), which may be explained by the presence of H-bonds within the composite structure. The diffraction spectrum of sample ‘b’ (CS 82%: DMAc 14%: AgNP/GO 4%) had three broad peaks at 2θ 21.5°, 24.7°, and 27.5°, which may be explained by Ag particles' enhanced hydrogen bond attraction to the membrane surface when DMAc concentration increased in the CS polymer membrane sample. AgNP is strongly attracted to the carbonyl groups of the CS-GO-DMAc chemical bonding, as evidenced by the sharp in sample ‘c’ (CS 78%: DMAc 18%: AgNP/GO 4%). A broader diffraction peak is noticed at 222.3°, with a sharp peak at 32.3°. Generally, all the samples displayed a steady disappearance of noticeable peaks after 35.0°, suggesting that the d-spacing gradually decreases, which may indicate the depletion of O-H functional groups near the membrane's edges [9]. So, the above observation may show that AgNP has been completely absorbed onto the surface of the modified chitosan (CS) matrix.

C. Modified CS thermogravimetric analysis ocument Modification

Thermogravimetric analysis (TGA) is a common method for examining the thermal decomposition properties of polymers. The TGA thermograms of CS, CS/DMAc, and CS/AgNP/GO/DMAc are shown in Figure 3.

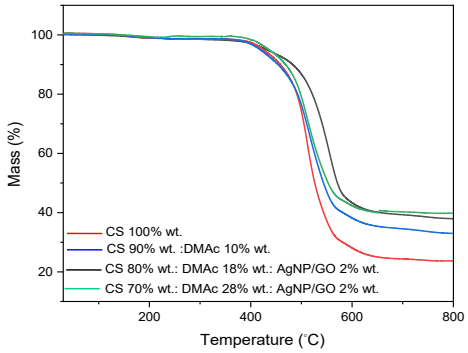

Fig. 3: TGA analysis of a modified CS composite

In general, all the composite membranes exhibited a relatively stable behavior between 30°C and 100°C, as evidenced by the absence of any noticeable weight loss. This stability is a result of CS's chemical composition. Prior to deterioration, chitosan (CS) requires a considerable quantity of thermal energy to break apart the intricate hydrogen bonds present in its molecular structure [10]. Figure 3 demonstrates that all composite samples exhibited a thermal degradation pattern comprised of two distinct phases. The first phase occurs between 100 °C and 380 °C and can be attributed to the partial eradication of the water molecule that was both adsorbed and bound. During the second stage, which occurred between 380°C and 620°C, the polymer underwent significant degradation, resulting in a weight loss of more than 80% of the modified CS polymer. This weight loss can be attributed to the disintegration of the polymer's molecular structures [10]. The difference in thermal stability between CS and CS/DMAc is primarily attributable to differences in their molecular weight and structural properties.

Due to the gradual increase in DMAc concentration and corresponding decrease in CS quantity, the modified composite exhibited enhanced thermal stability and decreased membrane weight loss. These results imply that DMAc has the potential to improve the thermal stability of CS membranes. Furthermore, the inclusion of AgNP-GO resulted in a modest reduction in weight loss to approximately 7% due to a further enhancement in thermal stability. The membrane samples' thermal stability may have been further improved by the incorporation of silver nanoparticles (AgNP) into the CS matrix [12].

D.Surface hydrophilicity

The measurement of the water contact angle is one of the most important ways to show how hydrophilic and wettable the surface of a modified CS membrane composite can be determined. Table 1 illustrates contact angle values for different components of modified chitosan. The influence of CS modification using DMAc, AgNP-GO, and the combination of all the components showed that the hydrophilicity of the modified CS matrix improved with the addition of DMAc. All the samples showed a gradual decline in the contact angle over the entire duration of 25 seconds, as shown in Figure 4. Among the modified CS matrix components, the CS/DMAc membrane has the highest contact angle of 85.7°, followed by CS/AgNP/GO (81.3°) and CS/AgNP/GO/DMAc (71.4°) after 5 seconds. The contact angle of the CS matrix further decreased after 25 seconds in this order: CS/DMAc (74.7°) > CS/AgNP/GO (61.9°) > CS/AgNP/GO/DMAc (47.3°). Previous studies have shown that proper blending of membrane composites would reduce contact and improve fluid transport [13].

TABLE 1: CONTACT ANGLE MEASUREMENT

Time (s)	CS/DMAc (°)	CS/AgNP/GO (°)	CS/AgNP/GO/DMAc (°)
5.0	85.7 ±0.3	81.3 ±0.4	71.4 ±0.3
10.0	83.5 ±0.2	72.7 ±0.2	65.2 ±0.5
15.0	81.2 ±0.1	70.0 ±0.3	58.3 ±0.2
20.0	77.0 ±0.3	64.2 ±0.2	52.9± 0.3
25.0	74.7 ±0.4	61.9 ±0.1	47.3 ±0.5

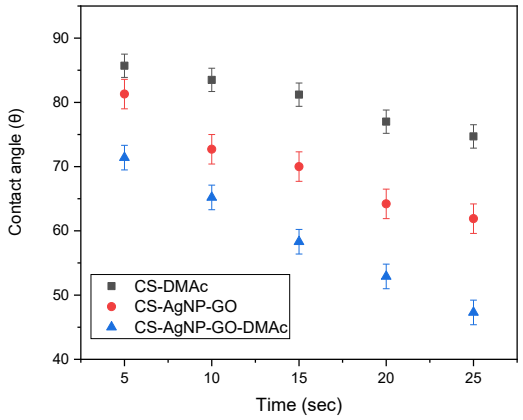

Fig. 4: Modified CS water contact angle measurements

It might be possible that DMAc, which was incorporated as a plasticizer, could make the composite membrane more water-friendly. This would lower the contact angle and make the surface of the modified CS membranes easier to wet [8]. Furthermore, stretching vibrations in the primary amino groups of CS, together with N-H bending of hydrogen-oxygen interaction (O-H) within the CS-DMAc-GO membrane network and C-O stretching of residual acetyl groups in CS, could have a strong affinity for water molecules, thereby reducing the contact angle and subsequently increasing the wettability of the CS/AgNP/GO/DMAc composite, as revealed by FT-IR. The presence of more hydroxyl groups in the composite may be responsible for promoting water molecules diffusion from the surface to the interior of the membrane composite, which could possibly bound water molecules through electrostatic and hydrogen bonding.

E. CS/AgNP/GO selectivity and antifouling performance

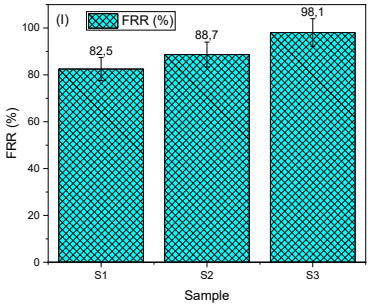

Fig. 4 (I): Flux recovery ratios (FRR)

The presence of contaminants on membranes has been widely recognized to have significant adverse consequences, including reduced membrane lifespan, diminished membrane separation resistance, and impaired membrane function [15]. The effectiveness of the composite membrane's ability to resist fouling was assessed by the quantification of the flow rate of a 100-parts-per million bovine serum albumin (BSA) solution subjected to a pressure of 0.25 MPa. Figure 4 (I) and (II) illustrate the antifouling properties of modified CS composites with the following compositions: S1 (CS 86%: DMAc 10%: AgNP/GO 4%); S2 (CS 82%: DMAc 14%: AgNP/GO 4%); and S3 (CS 78%: DMAc 18%: AgNP/GO 4%).

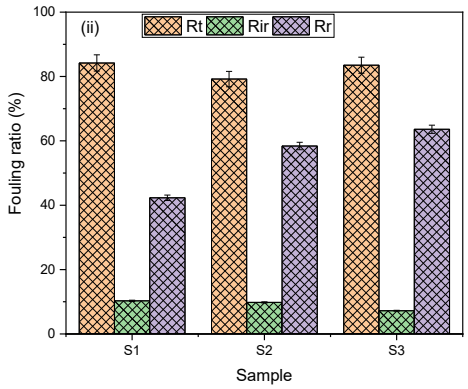

Fig. 4 (II): Antifouling behaviour of CS matrix

In Figure 4 (I), the flux recovery ratios (FRR) of the CS composite membranes after BSA filtration are shown so that the tendency of the membrane to get clogged up can be measured. A higher FRR value indicates a positive antifouling characteristic [46]. Notably, sample S1 (CS 86%: DMAc 10%: AgNP/GO 4%) demonstrated the lowest flux recovery ratio, while sample S3 (CS 78%: DMAc 18%: AgNP/GO 4%) exhibited the highest flux recovery rate of 98.1%. The ability of the modified CS composites to get wet and the presence of silver ions (Ag^+) on the membrane surface, which were probably surrounded by graphene oxide-epoxy clouds in the CS matrix, may have affected the flux recovery rates and the ability of these membranes to stay clean. Increased surface contact between the BSA and the membranes may be a potential explanation for the higher FRR observed in sample S3. The improved surface contact can be attributed to a greater abundance of -NH_2 groups from the DMAc group and -OH groups from the CS, which facilitated the binding of water molecules via electrostatic and hydrogen bonding interactions, which resulted in the formation of a dense layer of water molecules on the surface of the membrane, thereby increasing the affinity for the negatively charged BSA.

Figure 4 (II) shows how the reversible fouling ratio (Rr), the irreversible fouling ratio (Rir), and the total impurity ratio (Rt) were used to figure out the fouling resistance of composite membranes. The rise in the overall fouling ratio seen in sample S3 (CS/AgNP/GO-0.4%/DMAc) could be because the reversible fouling ratio (Rr) went up. The sample S3 composite exhibited a significant fouling prevention rate of over 79.6%. This may be because BSA molecules may come into contact with the surface of the membrane, which is rich in silver ions (Ag^+), which effectively stop contamination from happening on the membrane surface.

The reversible fouling (Rr) exhibited a high degree of backwashability; therefore, the flux recovery ratio of S3 exhibited the highest Rr value. Nevertheless, it is worth noting that samples S2 and S1 demonstrated comparatively lower Rr values, leading to a decrease in their FRR percentages. This outcome may be attributed to the substantial adsorption and deposition of contaminants on the membrane surface as well as the constriction of membrane pores. Furthermore, the percentages of irreversible fouling ratios (Rir) observed in all three samples were rather low, suggesting that they exhibited satisfactory antifouling properties against bovine serum albumin (BSA). As a result, the CS/AgNP/GO/DMAc membrane exhibited the most improved inhibition of fouling.

IV. CONCLUSION

The antifouling efficacy of CS/AgNP/GO membranes was dependent on the correct merging of membrane components and interaction with the BSA solute. Increased DMAc concentration and decreased CS mole ratio resulted in enhanced membrane wettability. Additionally, the membrane thermal stability was improved by the incorporation of DMAc and silver nanoparticles (AgNP) into the CS matrix, whereas the presence of more hydroxyl groups in the composite facilitated diffusion from the surface to the interior of the membrane composite via electrostatic and hydrogen bonding with water molecules.

ACKNOWLEDGMENT

The authors gratefully acknowledge the technical assistance and financial support provided by The Chemical Industries Education & Training Authority (CHIETA), and the Faculty of Engineering and Technology, Vaal University of Technology, Gauteng

REFERENCES

.

[1] D. Zhang, M.S. Sial, N. Ahmad, A.J. Filipe, P.A. Thu, M. Zia-Ud-Din, A.B. Caleiro, “Water Scarcity and Sustainability in an Emerging Economy: A Management Perspective for future. Sustainability”, 13 (2021), 144. https://doi.org/10.3390/su13010144

[2] Z. Fan., K.H.L. Po, K.K. Wong, S. Chen, S.P. Lau, “Polyethylenimine-modified graphene oxide as a novel antibacterial agent and its synergistic effect with daptomycin for methicillin-resistant Staphylococcus aureus,” ACS Appl. Nano Mater. 1 (2018), 1811–1818. https://doi.org/10.1021/acsanm.8b00219

[3] O. Agboola, O.S. Fayomi, A. Ayodeji, A.O. Ayeni, E.E. Alagbe, S.E. Sanni, E.E. Okoro, L. Moropeng, R. Sadiku, K.W. Kupolati, B.A Oni, “A review on polymer nanocomposites and their effective applications in membranes and adsorbents for water treatment and gas separation,” Membr. 11 (2021), 139. https://doi.org/10.3390/membranes11020139

[4] Z. Zou, B. Ismail, X. Zhang, Z. Yang, D. Liu, M. Guo, “Improving barrier and antibacterial properties of chitosan composite films by incorporating lignin nanoparticles and acylated soy protein isolate nanogel,” Food Hydro. 134 (2023), 108091 https://doi.org/10.1016/j.foodhyd.2022.108091

[5] J. Li, S. Zhuang, “Antibacterial activity of chitosan and its derivatives and their interaction mechanism with bacteria: Current state and perspectives.” J. Euro. Poly. 5 (2020), 109984. https://doi.org/10.1016/j.eurpolymj.2020.109984

[6] H. Karimi-Maleh, S. Ranjbari, B. Tanhaei, A. Ayati, Y. Orooji, M. Alizadeh, F. Karimi, S. Salmanpour, J. Rouhi, M. Sillanpa, “Novel 1-butyl-3-methylimidazolium bromide impregnated chitosan hydrogel beads nanostructure as an efficient nanobio-adsorbent for cationic dye removal: Kinetic study,” Enviro. Res. 195 (2021), 110809. https://doi.org/10.1016/j.envres.2021.110809

[7] H. Karimi-Maleh, S. Ranjbari, B. Tanhaei, A. Ayati, Y. Orooji, M. Alizadeh, F. Karimi, S. Salmanpour, J. Rouhi, M. Sillanpa, “Novel 1-butyl-3-methylimidazolium bromide impregnated chitosan hydrogel beads nanostructure as an efficient nanobio-adsorbent for cationic dye removal: Kinetic study,” Enviro. Res. 195 (2021), 110809. https://doi.org/10.1016/j.envres.2021.110809

[8] A.C. Ogazi, P.O. Osifo, “Effects of dimethylacetamide on chitosan/AgNP/GO fluid properties for 3D printing of water filtration membranes,” Polym. Adv. Technol. 34 (2023), 1220-1230.

[9] Y.M. Mohan, K. Vimala, V. Thomas, K. Varaprasad, B. Sreedhar, S.K. Bajpai, K.M. Raju, “Controlling of silver nanoparticles structure by hydrogel networks,” J. Colloid Interf. Sci. 342 (2010), 73 – 82 https://doi.org/10.1016/j.jcis.2009.10.008

[10] M.N. Pervez, G.K. Stylios, “Investigating the synthesis and characterization of a novel “green” H2O2-assisted, water-soluble chitosan/polyvinyl alcohol nanofiber for environmental end uses,” Nanomat. 8 (2018), 395. https://doi.org/10.3390/nano8060395

[11] Y.H. Khan, A. Islam, A. Sarwar, N. Gull, S.M. Khan, M.A. Munawar, S. Zia, A. Sabir, M. Shafiq, T. Jamil, “Novel green nano composites films fabricated by indigenously synthesized graphene oxide and chitosan,” Carbohy. Poly. 146 (2016), 131-138. https://doi.org/10.1016/j.carbpol.2016.03.031

[12] J.M. Quiroz-Castillo, D.E. Rodríguez-Félix, H. Grijalva-Monteverde, L.L. Lizárraga-Laborín, M.M. Castillo-Ortega, T. del Castillo-Castro, F. Rodríguez-Félix, P.J. Herrera-Franco, “Preparation and characterization of films extruded of polyethylene/chitosan modified with poly (lactic acid),” Mater. 8 (2014), 137-148. https://doi.org/10.3390/ma8010137

[13] S. Amiri, A. Asghari, V. Vatanpour, M. Rajabi, “Fabrication and Characterization of a Novel Polyvinyl Alcohol-Graphene Oxide-Sodium Alginate Nanocomposite Hydrogel Blended PES Nanofiltration Membrane for Improved Water Purification,” Sep. Purif. Technol. 250 (2020), 117216. https://doi.org/10.1016/j.seppur.2020.117216

[14] Y. Liu, L. Shen, Z. Huang, J. Liu, Y. Xu, R. Li, M. Zhang, H. Hong, H. Lin, “A novel insitu micro-aeration functional membrane with excellent decoloration efficiency and antifouling performance,” J. Membr. Sci. 641 (2022), 119925 https://doi.org/10.1016/j.memsci.2021.119925.